Biophysical Analyses of the Transthyretin Variants, Tyr114His and Tyr116Ser, Associated with Familial Amyloidotic Polyneuropathy†

Yoshinori Shinohara,‡ Mineyuki Mizuguchi,§ Kimiaki Matsubara,§ Makoto Takeuchi,§ Atsushi Matsuura,§ Takahiro Aoki,§ Kouhei Igarashi,§ Hatsumi Nagadome,‡ Yoshihiro Terada,*,‡ and Keiichi Kawano*,§

Faculty of Dental Science, Kyushu University, Fukuoka, Japan, and Faculty of Pharmaceutical Sciences, Toyama Medical and Pharmaceutical University, Toyama, Japan

Received July 30, 2003; Revised Manuscript Received September 19, 2003

ABSTRACT: The familial amyloidotic polyneuropathy is strictly associated with point mutations in the coding region of the transthyretin gene. Here, we focused on the mutations in the monomer−monomer and dimer−dimer interaction site of the transthyretin tetramer. The naturally occurring amyloidogenic Tyr114His (Y114H) and Tyr116Ser (Y116S) variants formed more amyloid fibrils than the wild-type transthyretin, nonamyloidogenic Tyr116Val (Y116V) variant, and other amyloidogenic variants in previous studies. The secondary, tertiary, and quaternary structural stabilities of the Y114H and Y116S variants were compared with those of the wild-type transthyretin and nonamyloidogenic Y116V variant. The unfolding data indicated that the amyloidogenic Y114H and Y116S mutations reduced the stability of the secondary, tertiary, and quaternary structure. Our results also indicated that the unfolding of Y114H and Y116S is less cooperative than that of the wild-type transthyretin. Moreover, the tetramer of the amyloidogenic variants dissociated to the monomer even at pH 7.0, indicating the importance of Tyr114 and Tyr116 in strengthening the contacts between monomers and/or dimers of the transthyretin molecule.

Transthyretin (TTR)[1] is a tetrameric human plasma protein (molecular mass 55 kDa) composed of identical 127-residue subunits, each having a β-sheet structure (*1*, *2*). TTR is encoded by a single copy gene on chromosome 18 and is secreted by hepatocytes into the blood serum, where it plays a major role in the transport of thyroxine and retinol, the latter via the TTR−retinol binding protein complex. In addition to hepatocytes, the retina and the choroid plexus of the brain are sites of synthesis for TTR (*3*−*6*).

TTR composes the amyloid fibrils found in patients afflicted with either familial amyloidotic polyneuropathy (FAP) or senile systemic amyloidosis (SSA) (*7*−*10*). Amyloid fibril formation refers to the deposition of an insoluble cross-β-sheet quaternary structure in the extracellular space which leads to degeneration of nerves and organ dysfunction. All experimental results in previous studies indicate that the amyloid fibrils found in patients with FAP and SSA are the causative agents of the diseases. The amyloid fibrils were found to be composed of normal transthyretin in patients with SSA, which affects approximately 25% of the population aged over 80 years (*11*, *12*). Deposition of TTR-derived amyloid in FAP patients is strictly associated with point mutations in the coding region of the TTR gene. Single point mutations in TTR are believed to enhance the amyloidogenicity of TTR and lead to FAP with the accumulation of amyloid in the peripheral nerves, kidney, spleen, heart, intestine, skin, and eye (*13*). The full-length TTR polypeptide is a predominant product of the amyloid fibrils in FAP patients, while fragments of TTR as well as full-length polypeptide are found in SSA amyloid deposits (*12*). The majority of FAP patients are heterozygous and therefore produce one copy of wild-type TTR for every copy of amyloidogenic variant TTR. The TTR tetramers in FAP patients are composed of wild-type and variant subunits; however, the amyloid fibrils are composed predominantly of variant TTR (*14*).

While the presence of an amyloidogenic mutation does not always lead to FAP, all of the early-onset FAP cases are associated with a TTR mutation, suggesting that the mutation is necessary but not sufficient for disease onset (*15*, *16*). The TTR structures of wild-type TTR and approximately 10 nonamyloidogenic and amyloidogenic variants have been solved by X-ray crystallography (*17*−*21*). However, these structures are identical with each other and provide no obvious clues to the molecular mechanisms of the amyloid fibril formation (*17*, *21*). Moreover, the FAP mutations are evenly distributed over the sequence, although the maximum mutational frequency is in the region of residues 45−58 encompassing the edge of the C- and D-strands (*22*). Therefore, neither the mutational positions in the primary sequence nor the slight structural changes due to the

† This study was supported by grants from the Ministry of Education, Culture, Sports, Science, and Technology of Japan, by the Program for the Promotion of Basic Research Activities for Innovative Biosciences (Japan), by the National Project on Protein Structural and Functional Analyses, and by a grant from the Ministry of Agriculture, Forestry, and Fisheries of Japan (Rice Genome Project PR-4101).

* Corresponding authors. Y.T.: tel, 81-92-642-6368; fax, 81-92-642-6374; e-mail, terada@dent.kyushu-u.ac.jp. K.K.: tel, 81-76-434-5061; fax, 81-76-434-5061; e-mail, kawano@ms.toyama-mpu.ac.jp.

‡ Kyushu University.

§ Toyama Medical and Pharmaceutical University.

[1] Abbreviations: TTR, transthyretin; FAP, familial amyloidotic polyneuropathy; SSA, senile systemic amyloidosis; SDS−PAGE, sodium dodecyl sulfate−polyacrylamide gel electrophoresis; CD, circular dichroism; OD, optical density.

10.1021/bi0353528 CCC: $25.00
Published on Web 12/02/2003

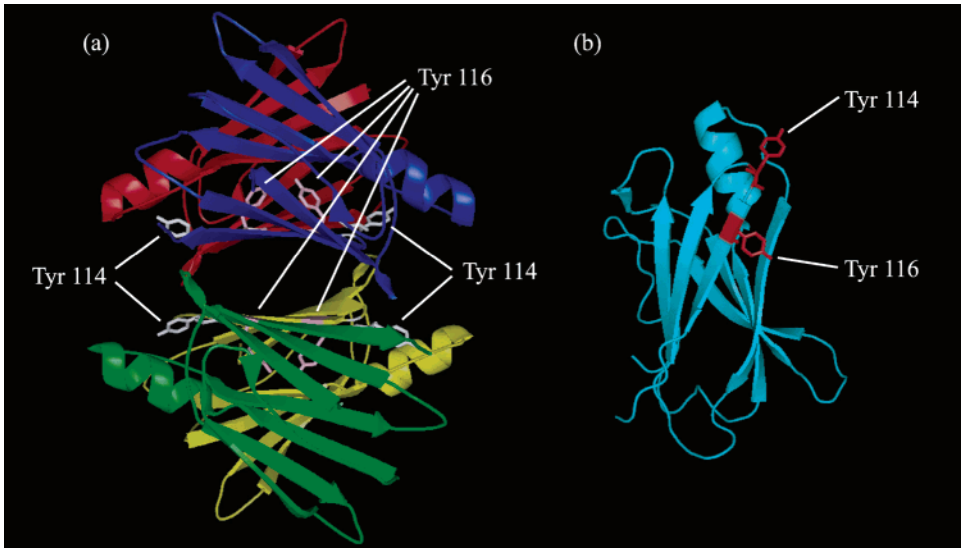

FIGURE 1: Ribbon diagrams of the tetrameric (a) and monomeric (b) TTR showing the aromatic side chains of the tyrosine residues at positions 114 and 116. The side chains of Tyr114 and Tyr116 are shown by a stick model. Tyr114 was mutated to the histidine residue, and Tyr116 was mutated to the serine and valine residues.

mutations reveal the molecular mechanisms underlying the amyloid fibril formation of TTR.

One of the basic models for fibril formation in FAP that has been established thus far was developed on the basis of a structural comparison of the amyloidogenic Met30 variant with wild-type TTR (*18*). Terry et al. (*18*) formulated a model based on the formation of a linear aggregate of TTR molecules linked by intermolecular disulfide bridges with the dimer as the basic building block. Another model is based on fibril formation from an amyloidogenic monomeric intermediate after partial acid denaturation (*23*−*26*). In in vitro studies, Kelly and Lansbury (*23*) demonstrated that TTR could self-assemble into amyloid-like fibrils in an acidic environment similar to that found in a lysosome. A third hypothesis was put forward which is based on the mutational frequency in the region of residues 45−58 encompassing the edges of the C- and D-strands (*22*). Triple mutant G53S/E54D/L55S TTR shows an altered local structure in this region and a novel protein packing arrangement, suggesting a double helix composed of two protein helices combined (*27*).

Extensive data support the hypothesis that single-site FAP-associated mutations destabilize the native protein fold, favoring dissociation and the formation of an alternatively folded monomeric amyloidogenic intermediate under conditions where the wild-type tetramer is stable. The formation of the amyloidogenic intermediate allows self-assembly and, ultimately, amyloid fibril formation (*23*, *28*−*33*). However, less than 10 of the TTR variants associated with FAP have been studied by biophysical methods so far, although more than 80 variants associated with FAP have been reported (*13*, *34*). Therefore, it is not yet clear whether the disease-associated mutations generally alter secondary and tertiary structural stability in addition to quaternary structural stability.

In the present study, we focus on the mutations in the monomer−monomer and dimer−dimer interaction site of the TTR molecule and report the secondary, tertiary, and quaternary structural stabilities of the naturally occurring amyloidogenic Tyr114His (Y114H) and Tyr116Ser (Y116S) variants, which are believed to cause TTR amyloidosis (*35*−*38*). We also studied the Tyr116Val (Y116V) variant, which has been found in healthy adult individuals (*39*), and compared it with the results of the Y114H and Y116S variants. Tyr114 is located in the loop between the G- and H-strands and is composed of parts of both monomer−monomer and dimer−dimer interfaces (Figure 1). Tyr116 in the H-strand is located in the monomer−monomer interface (*34*) (Figure 1). We demonstrated that the Y114H and Y116S variants were less stable and formed more amyloid fibrils than the wild-type TTR, Y116V, and FAP variants studied previously.

MATERIALS AND METHODS

Protein Expression and Purification. The expression plasmids of Y114H, Y116S, and Y116V TTR were prepared with the plasmid of wild-type TTR as a template using the QuikChange site-directed mutagenesis procedure from Stratagene (La Jolla, CA). The wild-type TTR and the variants were expressed and purified as described (*40*). The concentrations of proteins were determined by the absorbance at 280 nm, using an extinction coefficient of 71120 M^{-1} cm^{-1} for wild-type TTR and 66000 M^{-1} cm^{-1} for TTR variants.

Fibril Formation Assay. The fibril formation was studied as described previously (*41*). A TTR stock solution containing 1.0 mg/mL of proteins was diluted 1:1 with 200 mM citrate or phosphate buffer at the pH of interest. Citrate buffer was used when a final pH below 5.4 was desired; phosphate buffer was employed to evaluate amyloidogenesis at pH levels above 5.4. The turbidity measurements at 400 nm were carried out on a model UV-160A UV−visible spectrophotometer (Shimadzu). Thioflavin T binding was also used to evaluate the amyloid fibril formation in a pH range from 3.4 to 7.4 (*41*). The fibril solution (400 μL) was mixed with 2.75 mL of a buffer (50 mM Tris, 100 mM KCl, and 1 mM EDTA at pH 8.0), together with 30 μL of a thioflavin T stock solution (2.0 mM).

Monitoring pH-Induced Tetramer Dissociation of Wild-Type TTR and the Variants by SDS−PAGE. The TTR

solutions (0.2 mg/mL) at various pHs were incubated at 4 °C for 40 h. Ten microliters of the TTR solution was mixed with 5 μL of a gel-loading buffer containing 0.1% SDS and 13% glycerol. The samples were loaded on a 15% SDS−acrylamide gel without boiling. The fractions of monomer, dimer, and tetramer were quantified by densitometry using the program NIH IMAGE (*42*).

Urea-Induced Unfolding Monitored by Far-UV CD and Tryptophan Fluorescence. The protein solutions at pH 7.0 (0.4 mg/mL TTR) containing various concentrations of urea were incubated at 25 °C for 96 h before data collection (*41*). Concentrations of urea were determined by refractive index measurements (*43*, *44*). The temperature was maintained at 25 °C for all measurements. The far-UV CD and fluorescence spectra were recorded on a J-805 spectrometer (Jasco) and a F-4500 fluorescence spectrophotometer (Hitachi), respectively. The I_{355}/I_{335} ratio of the fluorescence intensity at 355 (exposed Trp) and 335 nm (buried Trp) was used to study the urea-induced unfolding (*41*).

Monitoring pH-Induced Unfolding of Wild-Type TTR and the Variants by Circular Dichroism. TTR solutions (100 mM phosphate or acetate, 200 mM KCl) at a protein concentration of 0.2 mg/mL and various pH levels were prepared at 0 °C and incubated at 4 °C for 48 h, since TTR does not aggregate at temperatures below 25 °C (*45*).

Size Exclusion Chromatography. Size exclusion chromatography was performed as described (*40*). The column was cleaned with 0.5 M NaOH and was equilibrated with 50 mM phosphate buffer (pH 7.0) containing 100 mM KCl and 1 mM EDTA before a protein solution was injected.

RESULTS

Extent of Wild-Type and Variant TTR Amyloid Fibril Formation as a Function of pH. The extent of wild-type TTR and variant amyloid fibril formation at 37 °C as a function of pH was monitored by turbidity at 400 nm between pH 3.4 and 7.4 (Figure 2a). The pH-dependent amyloidogenicities of wild-type TTR and the amyloidogenic variants (Y114H and Y116S) were not identical, with the Y114H and Y116S variants being able to self-assemble at higher pH values and over a broader range. The extent of wild-type and variant TTR amyloid fibril formation at 37 °C as a function of pH was also monitored by quantitative thioflavin T binding of the amyloid suspension (Figure 2b). Although the wild-type TTR and the variants did not exhibit turbidity at pH 3.4 (400 nm), suggesting the absence of large insoluble aggregates (Figure 2a), thioflavin T binding was observed after the incubation of wild-type TTR and the variants at pH 3.4 (Figure 2b). The apparent discrepancy between the thioflavin T binding and the turbidity assays at pH 3.4 may be explained by the presence of small oligomers at pH 3.4, at least some of which have an amyloid-like structure. To compare the relative amount of amyloid fibril formation between wild-type TTR and the variants, the ratio of OD at 400 nm for the variants to OD at 400 nm for wild-type TTR is represented in Figure 2c. The intensity ratio of thioflavin T fluorescence between wild-type TTR and the variants at various pHs is also shown in Figure 2d. As expected, good agreement is observed when comparing turbidity measurements and the thioflavin T binding as a measure of the relative amounts of amyloid fibril formation.

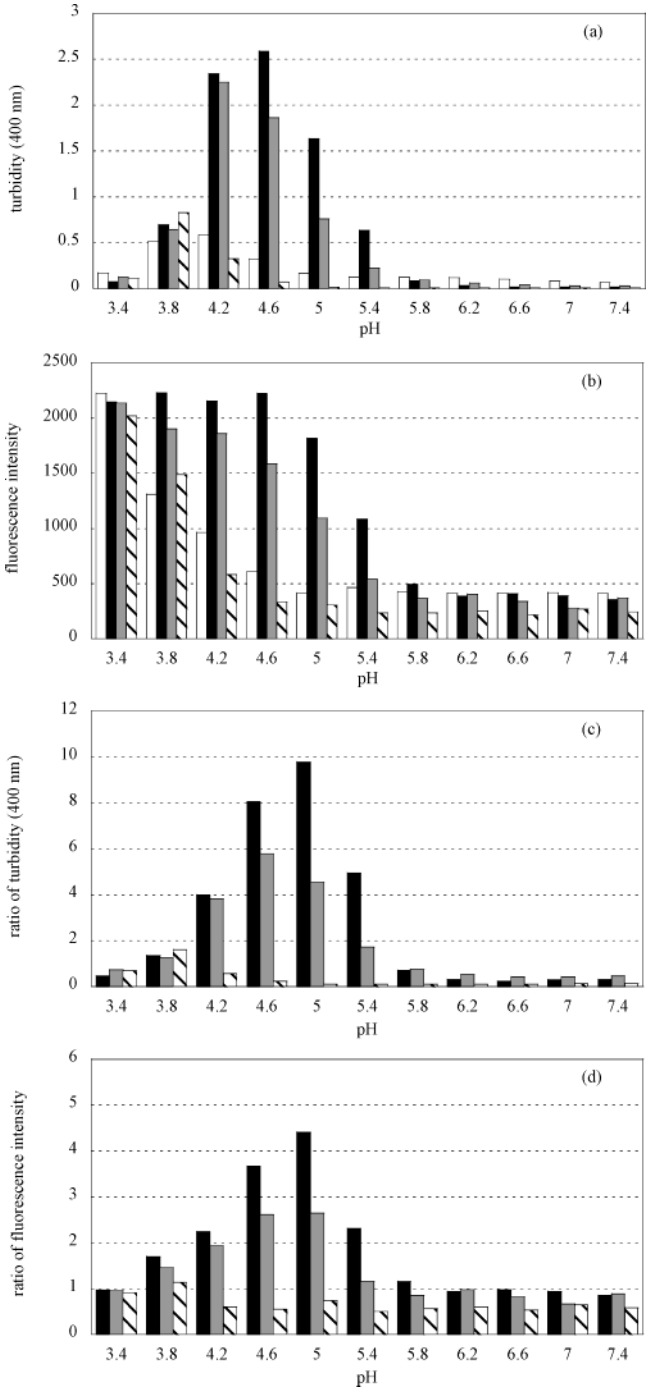

FIGURE 2: Fibril formation of wild-type TTR and the variants as a function of pH. The amount of amyloid fibril formed was evaluated by turbidity at 400 nm (a) and fluorescence intensity at 482 nm in thioflavin T binding assay (b). Samples were incubated at 37 °C for 72 h before the assay. White, black, dotted, and hatched bars represent wild-type, Y114H, Y116S, and Y116V TTR, respectively. The intensity ratio between wild-type TTR and the variants at various pHs derived from the data of turbidity (c) and thioflavin T fluorescence (d). Black, dotted, and hatched bars represent the intensity ratio of Y114H, Y116S, and Y116V to wild-type TTR, respectively.

The Y114H and Y116S variants formed more amyloid fibrils than wild-type TTR, while the extent of the fibril formation of the Y116V variant was similar to that of wild-type TTR (Figure 2c,d).

Quaternary Structural Stabilities of Wild-Type TTR and Variants Monitored by SDS−PAGE. Wild-type TTR is

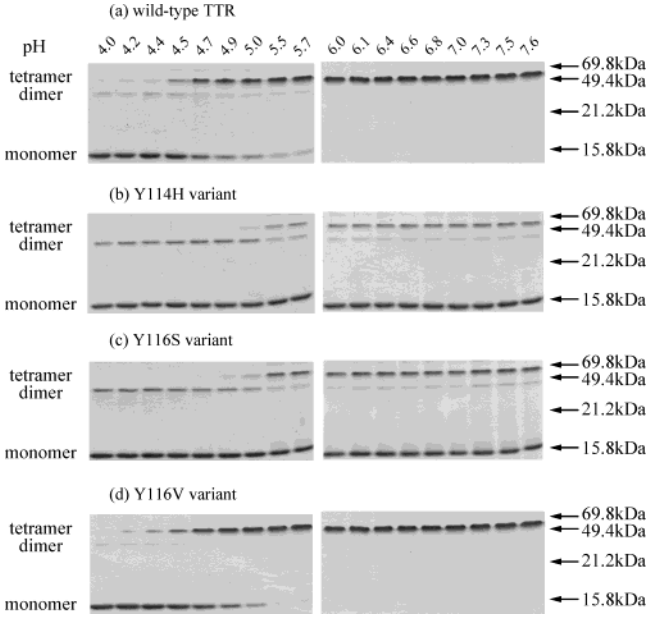

FIGURE 3: Photograph of SDS−PAGE gels showing tetramer-to-monomer transitions of wild-type TTR and variants. The samples at various pHs were incubated at 4 °C for 40 h and subjected to SDS−PAGE.

known to retain the tetrameric or dimeric structure after denaturation with SDS and run as the tetramer or dimer on an SDS−PAGE gel (*25*, *28*, *29*, *45*−*48*). The samples at pH 7.0 for wild-type and Y116V TTR showed the band corresponding to the tetramer, while the bands corresponding to the tetramer, dimer, and monomer were observed for Y114H and Y116S variants at pH 7.0 (Figure 3). These results are consistent with the data of analytical size exclusion chromatography at pH 7.0 (see below). Previous studies have shown that the acid-induced tetramer-to-monomer equilibrium can be monitored by SDS−PAGE (*25*, *28*, *29*, *45*−*47*). The Y114H and Y116S variants showed the strong band corresponding to the monomer at all pH values studied, whereas the wild-type and Y116V TTR showed the monomeric band below pH 4.9 (Figure 3). These data indicate that the substitution of Tyr116 with Val does not perturb the stability of the quaternary structure and that the tetramers of the amyloidogenic variants (Y114H and Y116S) are destabilized relative to wild-type TTR under these experimental conditions.

Monitoring pH-Induced Unfolding of Wild-Type TTR and Variants by Circular Dichroism. To evaluate the conformational changes occurring in TTR as a function of pH, near-UV CD studies were employed to probe the tertiary structural changes. The CD ellipticity at 291 nm, resulting from the asymmetric packing of the tryptophan side chains, reveals significant pH-dependent tertiary structure changes (Figure 4). The CD signal of wild-type TTR from pH 7.0 to pH 5.5 exhibited little change, showing a largely unchanged tertiary structure over this pH range. The signal became less intense over the amyloid-forming pH range of 5.0−4.2, implying a change in tertiary structure over this pH range. Whereas the tryptophan near-UV CD signals of the Y114H and Y116S variants gradually decreased over the pH range of 7.0−4.2 (Figure 4a,b), only a slight decrease in intensity of the CD signal for the Y116V variant was detected in the same pH range (Figure 4c). Below pH 4.0, the CD signal at 291 nm

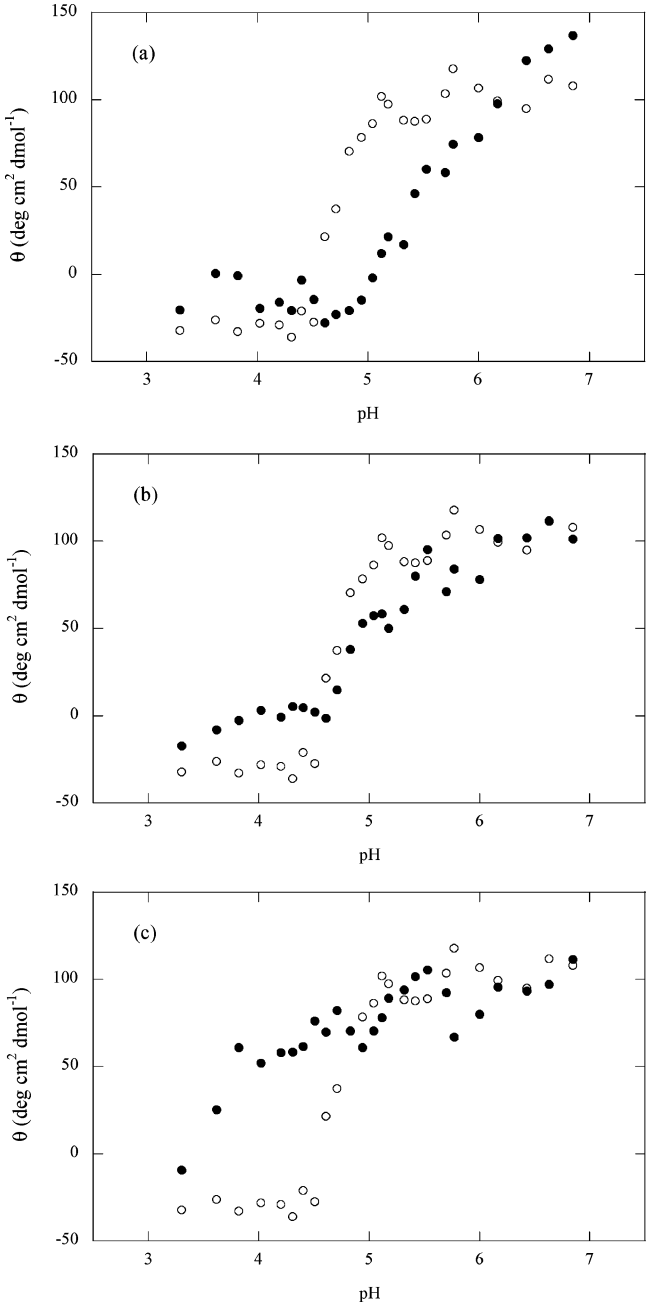

FIGURE 4: Acid denaturation of wild-type TTR and the variants monitored by changes in the CD ellipticities at 291 nm. All samples (0.2 mg/mL) at various pHs were incubated at 4 °C for 48 h before measurement. Filled symbols designate the data of the Y114H (a), Y116S (b), and Y116V (c) variants. The data of wild-type TTR are represented by open symbols for comparison.

almost disappeared, which indicates a rearranged and poorly defined tertiary structure of wild-type TTR and amyloidogenic variants. The tertiary structures of the amyloidogenic variants (Y114H and Y116S) are more sensitive to acidic conditions than is wild-type TTR, and the non-amyloidogenic variant (Y116V) is the most stable among the four proteins at the pH range studied.

Urea-Induced Unfolding of Wild-Type TTR and the Variants Monitored by Far-UV CD and Trp Fluorescence. Urea-induced equilibrium unfolding of wild-type TTR and the variants was investigated by Trp fluorescence spectroscopy and by the CD at 215 nm. The apparent fractional extent of unfolding, f_{app}, was calculated from the values of the CD at

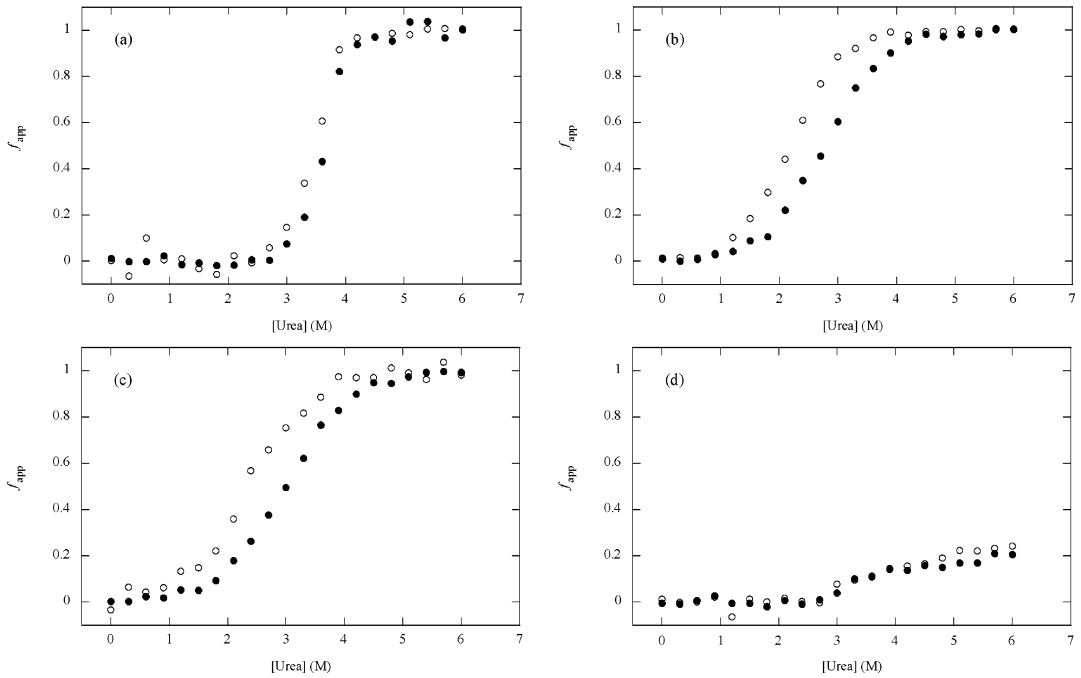

FIGURE 5: Apparent fractional extent of unfolding, f_{app}, of wild-type TTR (a) and the Y114H (b), Y116S (c), and Y116V (d) variants calculated from the ellipticity values at 215 nm (open symbols) and I_{355}/I_{335} (filled symbols). The baselines of the posttransition zone for Y116V are assumed to be the same as those for wild-type TTR.

Table 1: Stability Parameters of Wild-Type TTR and the Variants Calculated from the Data on Urea-Induced Unfolding[a]

	C_m[b] (M)	m[b] (kcal mol^{-1} M^{-1})	C_m[c] (M)	m[c] (kcal mol^{-1} M^{-1})
wild type	3.50 ± 0.02	2.50 ± 0.23	3.50 ± 0.01	2.84 ± 0.18
Y114H	2.19 ± 0.01	1.36 ± 0.02	2.76 ± 0.01	1.16 ± 0.02
Y116S	2.37 ± 0.03	1.10 ± 0.05	2.99 ± 0.01	1.06 ± 0.02
Y116V	ND[d]	ND[d]	ND[d]	ND[d]

[a] The C_m values represent the denaturant concentrations at the midpoint of the urea-induced unfolding curves shown in Figure 5. The m values represent the cooperativity indices of the unfolding. [b] Derived from the unfolding curves monitored by CD ellipticities at 215 nm. [c] Derived from the unfolding curves monitored by the fluorescence intensity ratio (I_{355}/I_{335}). [d] Not determined.

215 nm and the I_{355}/I_{335} ratio by the equation $f_{app} = (A_{obs} - A_1)/(A_2 - A_1)$, where A_1 and A_2 represent the baselines for the pre- and posttransition zone, respectively, and A_{obs} is the observed CD value or I_{355}/I_{335} ratio (Figure 5). Table 1 shows the denaturant concentration at the midpoint of the unfolding (C_m) and the cooperativity index of the unfolding (apparent m value) obtained from the curves in Figure 5.

Resistance of the TTR Variants to Dissociation into Monomers at pH 7.0. To characterize in detail the equilibrium in solution for wild-type TTR and the variants (Y114H, Y116S, and Y116V), we ran gel filtration experiments at various protein concentrations. Figure 6 shows the gel filtration elution profiles of four different proteins at pH 7.0 at four different protein concentrations between 0.2 and 1.0 mg/mL. Peaks corresponding to different molecular species in solution were observed with apparent molecular masses in the following order: 60 kDa for the tetramer (elution volume = 10.4 mL) and 15 kDa for the monomer (elution volume = 13.1 mL). For wild-type TTR (Figure 6a), most of the protein was in the tetrameric form at 1.0 mg/mL. A similar behavior was observed for the Y116V variant (Figure 6d). In the case of the Y116S variant, most of the protein was in the tetrameric form, but small amounts of the monomer were observed at 1.0 mg/mL (Figure 6c). For the Y114H variant at 1.0 mg/mL (Figure 6b), a broad peak was observed with an exclusion volume corresponding to a level between the tetrameric form and the monomeric form, indicating rapid equilibrium between the different molecular species or a range of conformations with different exclusion volumes. Thus, two amyloidogenic mutations Y114H and Y116S lead to dissociation of the tetramer at pH 7.0. Additionally, the dilution leads to dissociation of the tetramer to monomer for the Y116S variant, since the fraction of monomer increased as the protein concentration decreased (Figure 6c). However, in the case of the Y114H variant, the broad peak was observed in a wide range of protein concentrations (Figure 6b). There was no monomeric form of wild-type TTR or the Y116V variant in the protein concentration range studied (Figure 6a,d). Therefore, the wild-type TTR and the Y116V tetramer are more stable to dissociation than the two amyloidogenic TTR variants at pH 7.0.

DISCUSSION

The amyloidogenic potential of certain amino acid substitutions in TTR is not predictable, and the severity and onset of symptomatic TTR amyloidosis remain an empirical clinical observation. Therefore, it is important to understand the precise causes and mechanisms responsible for aberrant TTR subunit assembly or misassembly into amyloid fibrils. Comparative studies of the native fold and abnormal conformations of TTR are expected to be useful in developing therapeutic strategies for intervention in amyloid disease.

We studied naturally occurring amyloidogenic variants, the Y114H and Y116S variants, in which the Tyr114 and Tyr116 residues were substituted with His and Ser, respectively. The patient who had the Y114H variant was clinically characterized by generalized cutaneous amyloid deposits and

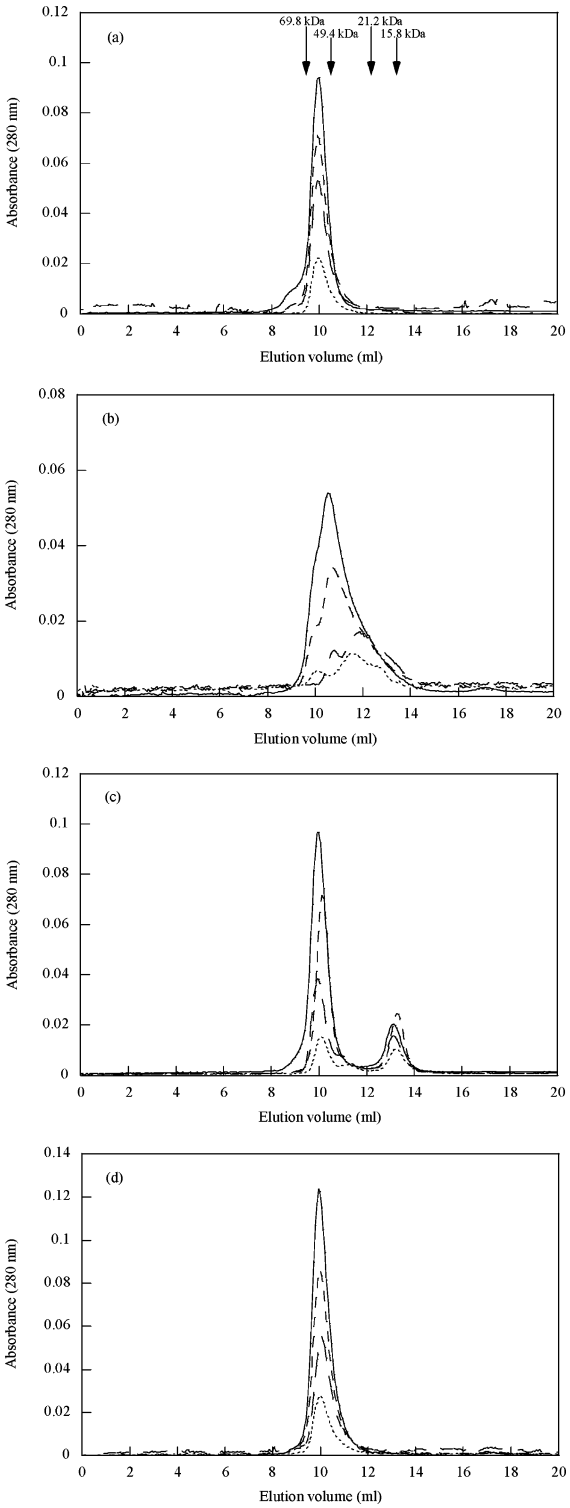

FIGURE 6: Analytical size exclusion chromatograms of wild-type TTR (a) and the Y114H (b), Y116S (c), and Y116V (d) variants. The samples at various protein concentrations were incubated at 4 °C for 12 h and subjected to size exclusion chromatography. All chromatograms were run at a flow rate of 0.4 mL/min at 4 °C. Solid, broken, broken dash, and dotted lines represent the gel filtration chromatograms at protein concentrations of 1.0, 0.6, 0.4, and 0.2 mg/mL, respectively. The protein standards used to calibrate the molecular masses are albumin (69.8 kDa), ovalbumin (49.4 kDa), chymotrypsinogen A (21.2 kDa), and ribonuclease A (15.8 kDa).

late-onset carpal tunnel syndrome (CTS) with a lack of overt polyneuropathy and autonomic dysfunction (*35*, *38*). The Y116S mutations were detected in patients with amyloidosis, and the patient who had the Y116S variant presented with axonal sensory neuropathy and a bilateral carpal tunnel syndrome (*36*, *37*). We also studied the structure and stability of the nonamyloidogenic Y116V variant, found in healthy adult individuals, in which Tyr116 was substituted with Val (*39*). Our results showed that the amino acid substitutions of Tyr114 to His and Tyr116 to Ser result in substantial destabilization of the TTR molecule and make the TTR molecule more amyloidogenic. On the other hand, the amino acid substitution of Y116 to Val stabilized the secondary and tertiary structure, although the quaternary structure was not affected (Figures 2−6).

To compare the relative amyloidogenicity of the Y114H, Y116S, and Y116V variants with wild-type TTR and with the variants studied previously, we followed the experimental methods used in previous investigations (*25*, *41*, *45*, *46*, *49*−*51*). Wild-type TTR is converted into amyloid by pH-mediated tetramer dissociation coupled with tertiary structural changes, resulting in the formation of a so-called monomeric amyloidogenic intermediate that self-assembles into amyloid fibrils (*45*). Previous study has demonstrated that the V122I variant forms 1.2- and 1.7-fold more amyloid fibrils than wild-type TTR at pH 4.2 as judged by turbidity and thioflavin T binding, respectively (*46*). The L55P variant has been shown to form approximately 1.5-fold more amyloid fibrils than wild-type TTR, whereas the extent of amyloid formation of the V30M variant is equivalent to that of wild-type TTR as judged by turbidity (*25*, *49*). Our results show that the Y114H variant forms 10-fold more fibrils than wild-type TTR as judged by turbidity and 4.5-fold more fibrils as judged by thioflavin T binding (Figure 2c,d). The Y116S TTR forms 6-fold more fibrils than wild-type TTR as judged by turbidity and 2.5-fold more as judged by thioflavin T binding (Figure 2c,d). Therefore, the Y114H and Y116S variants are more amyloidogenic than the V30M, L55P, and V122I variants studied in previous studies (*25*, *46*, *49*). These characteristics can be explained by the destabilization of the tetramer of Y114H and Y116S, since these variants readily dissociate to monomer in the presence of a low concentration of SDS at pH 7.0 (Figure 3). The tetramer−monomer equilibrium analyzed by SDS−PAGE in previous studies indicated that the V30M, L55P, and V122I variants can form tetramers at pH 6.0−7.0 in the presence of a low concentration of SDS (*25*, *29*, *46*). The instability of the tetramer for the Y114H and Y116S variants is also evident from the data of analytical size exclusion chromatography (Figure 6b,c). At 4 °C and pH 7.0, the Y114H and Y116S variants (1.0 mg/mL) seem to exist as a mixture of tetramer, dimer, and monomer, since the Y114H variant shows a broad peak and the Y116S variant shows two peaks corresponding to the tetramer and the monomer. In contrast, the wild-type TTR and the Y116V variant (1.0 mg/mL) showed only a single and symmetrical peak at the position corresponding to the tetramer. The amyloidogenic Y116S variant showed that the native tetrameric form dissociates to monomeric species depending on protein concentration at pH 7.0 (Figure 6c). The tetramer of wild-type TTR and the nonamyloidogenic TTR variant (Y116V) never dissociated to monomer upon dilution in the range of 0.2−1.0 mg/mL, indicating higher stability of the tetramer. Our results showed that two forms of Y116S coexisted in solution at a 1.0 mg/mL protein concentration. Eighty-five percent of the molecules were in

the tetrameric form and 15% in the monomeric form at a protein concentration of 1.0 mg/mL (Figure 6c). When the Y116S solution is diluted 4-fold, the fractions of tetramer and monomer were altered to 60% and 40%, respectively. When a hydrophilic amino acid is introduced at the position of Tyr116, the GH loop may become looser and disconnected from the body of the tetramer. The substitution of Tyr114 to His resulted in the destabilization of the tetramer at 0.2−1.0 mg/mL, since the broad peak was observed in gel filtration chromatography (Figure 6b). The Tyr114 residue, deep in the hydrophobic core of the tetramer, is located in the monomer−monomer interface (Figure 1a). The substitution of Tyr114 with a charged histidine residue may disrupt or affect a number of noncovalent bonds. Therefore, the GH loop seems to represent one of the key structural elements for stabilizing the tetramer, since the amino acid substitution affects the stability of the tetramer, leading to dissociation into monomers. These results, with regard to the susceptibility of the amyloidogenic variants to dissociate, indicate the importance of Tyr114 and Tyr116 in strengthening the contacts between monomers and/or dimers.

The concentration of TTR in the serum ranges between 0.17 and 0.42 mg/mL (*52*), and TTR protein has been believed to exist as a stable tetrameric form in vivo. However, the tetramer-to-monomer dissociation process may occur and lead to the accumulation of monomeric species in some tissues. Some monomeric species may be potentially amyloidogenic, allowing aggregate formation and amyloid fibril growth (*24*). Therefore, the amyloidogenic potential of TTR variants studied here could be related to different tendencies of their monomeric species to be converted into monomeric amyloidogenic intermediates, which in turn could self-aggregate and eventually form amyloid fibrils.

The wild-type TTR and the Y114H and Y116S variants showed a urea-induced unfolding transition, but the Y116V variant was not induced to unfold by urea, showing that the Y116V substitution substantially stabilizes the TTR molecule (Figure 5). The C_m values measured by CD at 215 nm and Trp fluorescence for wild-type TTR are identical, showing the cooperative unfolding of wild-type TTR. However, the noncoincidence of C_m values measured by different methods is apparent for the amyloidogenic Y114H and Y116S variants (Table 1). This may indicate the noncooperative unfolding of the Y114H and Y116S structures (*53*−*55*). Noncooperative interactions in the amyloidogenic variants are also evident from the acid-induced unfolding monitored by CD at 291 nm, since the unfolding transitions of the Y114H and Y116S variants are less cooperative compared with the wild-type TTR (Figure 4). The C_m values of the Y114H and Y116S variants are lower than that of the wild-type TTR, showing that the amyloidogenic Y114H and Y116S mutations reduced the stability of the secondary and tertiary structure (Table 1).

In conclusion, our data indicate that the amyloidogenic mutations in the monomer−monomer and dimer−dimer interaction site perturb the stability of the secondary, tertiary, and quaternary structure (Figures 2−6 and Table 1). Therefore, the different in vivo behavior between amyloidogenic TTR variants and wild-type TTR may be mostly mediated by the differences in the secondary and tertiary structural stabilities of the monomers formed upon tetramer dissociation. The structure, stability, and dynamics of monomeric species may play a crucial role in the self-assembly and amyloidogenesis of TTR.

REFERENCES

1. Blake, C. C. F., Geisow, M. J., Swan, I. D. A., Rerat, C., and Rerat, B. (1974) *J. Mol. Biol. 88*, 1−12.
2. Blake, C. C. F., Geisow, M. J., and Oatley, S. J. (1978) *J. Mol. Biol. 121*, 339−356.
3. Raz, A., Shiratori, T., and Goodman, D. S. (1970) *J. Biol. Chem. 245*, 1903−1912.
4. van Jaarsveld, P. P., Edelhoch, H., Goodman, D. S., and Robbins, J. (1973) *J. Biol. Chem. 248*, 4698−4705.
5. Nilsson, S. F., Rask, L., and Peterson, P. A. (1975) *J. Biol. Chem. 250*, 8554−8563.
6. Yen, C., Costa, R. H., Darnell, J. E., Chen, J., and van Dyke, T. A. (1990) *EMBO J. 9*, 869−878.
7. Benson, M. D. (1989) *Trends Neurosci. 12*, 88−92.
8. Benson, M. D., and Uemichi, T. (1996) *Amyloid 3*, 44−56.
9. de Carvalho, M., Moreira, P., Evangelista, T., Ducha-Soares, J. L., Bento, M., Fernandes, R., and Saraiva, M. J. (2000) *Muscle Nerve 23*, 1016−1021.
10. Rochet, J. C., and Lansbury, P. T. (2000) *Curr. Opin. Struct. Biol. 10*, 60−68.
11. Cornwell, G. C., Sletten, K., Johansson, B., and Westermark, P. (1988) *Biochem. Biophys. Res. Commun. 154*, 648−653.
12. Westermark, P., Sletten, K., Johansson, B., and Cornwell, G. G. (1990) *Proc. Natl. Acad. Sci. U.S.A. 87*, 2843−2845.
13. Connors, L. H., Richardson, A. M., Theberge, R., and Costello, C. E. (2000) *Amyloid 7*, 54−69.
14. Gustavsson, A., Jahr, H., Tobiassen, R., Jacobson, D. R., Sletten, K., and Westermark, P. (1995) *Lab. Invest. 73*, 703−708.
15. Jacobson, D. R., and Buxbaum, J. N. (1991) *Adv. Hum. Genet. 20*, 69−123.
16. Saraiva, M. J. (1995) *Hum. Mutat. 5*, 191−196.
17. Schormann, N., Murrel, R. J., and Benson, D. M. (1998) *Amyloid 5*, 175−187.
18. Terry, C. J., Damas, A. M., Oliveria, P., Saraiva, M. J. M., Alves, I. L., Costa, P. P., Matias, P. M., Sakaki, Y., and Blake, C. C. F. (1993) *EMBO J. 12*, 735−741.
19. Sebastiao, M. P., Saraiva, M. J., and Damas, A. M. (1998) *J. Biol. Chem. 273*, 24715−24722.
20. Sebastiao, M. P., Merlini, G., Saraiva, M. J., and Damas, A. M. (2000) *Biochem. J. 351*, 273−279.
21. Hörnberg, A., Eneqvist, T., Olofsson, A., Lundgren, E., and Sauer-Eriksson, A. E. (2000) *J. Mol. Biol. 302*, 649−669.
22. Serpell, L. C., Goldsteins, G., Dacklin, I., Lundgren, E., and Blake, C. C. F. (1996) *Amyloid 3*, 75−85.
23. Kelly, J. W., and Lansbury, P. T. J. (1994) *Amyloid 1*, 186−205.
24. Quintas, A., Saraiva, M. J. M., and Brito, M. M. (1997) *FEBS Lett. 418*, 297−300.
25. Lashuel, H. A., Wurth, C., Woo, L., and Kelly, J. W. (1999) *Biochemistry 38*, 13560−13573.
26. Quintas, A., Vaz, D. C., Cardoso, I., Saraiva, M. J., and Brito, R. M. (2001) *J. Biol. Chem. 276*, 27207−27213.
27. Eneqvist, T., Andersson, K., Olofsson, A., Lundgren, E., and Sauer-Eriksson, A. E. (2000) *Mol. Cell 6*, 1207−1218.
28. McCutchen, S. L., Colon, W., and Kelly, J. W. (1993) *Biochemistry 32*, 12119−12127.
29. McCutchen, S. L., Lai, Z., Miroy, G. J., Kelly, J. W., and Colon, W. (1995) *Biochemistry 34*, 13527−13536.
30. Jenne, D. E., Denzel, K., Blatzinger, P., Winter, P., Obermaier, B., Linke, R. P., and Altland, K. (1996) *Proc. Natl. Acad. Sci. U.S.A. 93*, 6302−6307.
31. Kelly, J. W. (1996) *Curr. Opin. Struct. Biol. 6*, 11−17.
32. Kelly, J. W. (1998) *Curr. Opin. Struct. Biol. 8*, 101−106.
33. Lashuel, H. A., Lai, Z., and Kelly, J. W. (1998) *Biochemistry 37*, 17851−17864.
34. Eneqvist, T., and Sauer-Eriksson, A. E. (2001) *Amyloid 8*, 149−168.
35. Murakami, T., Tachibana, S., Endo, Y., Kawai, R., Hara, M., Tanase, S., and Ando, M. (1994) *Neurology 44*, 315−318.
36. Misrahi, A. M., Plante, V., Lalu, T., Serre, L., Adams, D., Lacroix, D. C., and Said, G. (1998) *Hum. Mutat. 12*, 71.
37. Plante-Bordeneuve, V., Lalu, T., Misrahi, M., Reilly, M. M., Adams, D., Lacroix, C., and Said, G. (1998) *Neurology 51*, 708−714.

38. Mochizuki, H., Kamakura, K., Masaki, T., Hirata, A., Tokuda, T., Yazaki, M., Motoyoshi, K., and Ikeda, S. (2001) *Amyloid 8*, 105−110.
39. Strahler, J. R., Rosenblum, B. B., and Hanash, S. M. (1987) *Biochem. Biophys. Res. Commun. 148*, 471−477.
40. Matsubara, K., Mizuguchi, M., and Kawano, K. (2003) *Protein Expression Purif. 30*, 55−61.
41. Jiang, X., Smith, C. S., Petrassi, M., Hammarstrom, P., White, J. T., Sacchettini, J. C., and Kelly, J. W. (2001) *Biochemistry 40*, 11442−11452.
42. Seebacher, T., and Bade, E. G. (1996) *Electrophoresis 17*, 1573−1574.
43. Krivacic, J. R., and Urry, D. W. (1971) *Anal. Chem. 43*, 1508−1510.
44. Pace, C. N. (1986) *Methods Enzymol. 131*, 266−280.
45. Lai, Z., Colon, W., and Kelly, J. W. (1996) *Biochemistry 35*, 6470−6482.
46. Jiang, X., Buxbaum, J. N., and Kelly, J. W. (2001) *Proc. Natl. Acad. Sci. U.S.A. 98*, 14943−14948.
47. Colon, W., and Kelly, J. W. (1992) *Biochemistry 31*, 8654−8660.
48. Furuya, H., Nakazato, M., Saraiva, M. J., Costa, S. P., Sasaki, H., Matsuo, H., Goto, I., and Sakaki, Y. (1989) *Biochem. Biophys. Res. Commun. 163*, 851−859.
49. Hammarstorm, P., Jiang, X., Hurshman, A. R., Powers, E. T., and Kelly, J. W. (2002) *Proc. Natl. Acad. Sci. U.S.A. 99*, 16427−16432.
50. Redondo, C., Damas, A. M., and Saraiva, M. J. M. (2000) *Biochem. J. 348*, 167−172.
51. Sekijima, Y., Hammarstorm, P., Matsumura, M., Shimizu, Y., Iwata, M., Tokuda, T., Ikeda, S., and Kelly, J. W. (2003) *Lab. Invest. 83*, 409−417.
52. Vatassery, G. T., Quach, H. T., Smith, W. E., Benson, B. A., and Eckfeldt, J. H. (1991) *Clin. Chim. Acta 197*, 19−25.
53. Kuwajima, K. (1989) *Proteins 6*, 87−103.
54. Kim, P. S., and Baldwin, R. L. (1990) *Annu. Rev. Biochem. 59*, 631−660.
55. Ptitsyn, O. B. (1995) *Adv. Protein Chem. 47*, 83−229.

BI0353528